

# Identification and Dynamic Inversion-Based Control of a Pressurizer at the Paks NPP

Zoltán Szabó, Gábor Szederkényi, Péter Gáspár, István Varga, Katalin M. Hangos, József Bokor

*Computer and Automation Research Institute, Hungarian Academy of Sciences  
Kende u. 13-17, H-1111 Budapest, Hungary;  
Fax: (+36-1) 466-7503; Phone: (+36-1) 279-6171; E-mail: gaspar@sztaki.hu*

---

## Abstract

This paper presents the design of a pressure controlling tank located in the primary circuit of a Nuclear Power Plant. All steps from the modeling through control design to the implementation are detailed. Based on first engineering principles a second order Wiener model is formulated and its unknown parameters are identified. The control design is based on a dynamic inversion method. The performance of the closed-loop system is tuned by an error feedback. The implemented controller has a distributed structure including measurement and control PLCs, a continuous power controller and a special supervisor module. The nominal stability of the controller in the networked environment is analyzed by using the maximum allowable transmit interval. The hardware and software design and implementation obey the safety-critical requirements imposed by the special nature of the plant.

*Keywords:* safety-critical systems, robust control, model identification, networked control, dynamic inversion, nuclear power plant.

---

## 1. Introduction

The continuously increasing (and sometimes conflicting) demands related to the safer, more effective and environmentally more friendly operation of complex plants often necessitates the reconstruction or even complete re-design of different subsystems. In many cases, the simplest (and cheapest) way to substantially influence important dynamical processes is the detailed modeling and model-based advanced feedback design for the affected components

of the system. One example for such a procedure is the successful modeling, identification and dynamic inversion based controller design for stabilizing the primary circuit pressure at the Paks Nuclear Power Plant in Hungary in 2004-2005 (see, e.g. [27], [31]). This controller implementation (together with other important reconstruction steps) largely contributed to the possibility that the average thermal power of the plant units could be increased by 1-2%. The implemented controller is a redundant networked control system (NCS), where the measurement results and the control commands are transferred to the computing units and actuators through an Ethernet network.

The Paks Nuclear Power Plant belongs to the group of Pressurized Water Reactors (PWRs). It was founded in 1976 and started its operation in 1981. The plant operates four VVER-440/213 type reactor units with a total nominal (electrical) power of 1860 MWs. About 40 percent of the electrical energy generated in Hungary is produced here. Considering the load factors, the Paks units belong to the leading ones in the world and have been among the top twenty-five units for years. The reconstructions included retrofitting some control loops that were designed and put into operation in the 1980's. As we will see later, the pressurizer and the corresponding pressure controller have key importance in maintaining the operation of the power plant.

The aim of this paper is to briefly describe the whole engineering design process from the physical modeling of the equipment through the identification and controller design steps to the safety critical implementation of the control loop.

The outline of the paper is as follows. Section 2 contains the brief description of the process modeling procedure, and section 3 is devoted to the model identification problem. The dynamic inversion based controller design and the performance analysis of the networked control loop are presented in sections 4 and 5, respectively. The implementation issues and results are summarized in section 6, and finally, section 7 contains the most important conclusions.

## **2. Process modeling**

### *2.1. Modeling goal and background*

Modeling of industrial vaporizers, expansion tanks and alike depends heavily on the modeling goal. Most of the commercially available dynamic models are implemented in

steady-state or dynamic simulators (see e.g. [1]) and are used for equipment design and retrofitting purposes. The models used for these purposes are typically in the form of partial differential equations that are discretized in space to have a lumped version. This way a high dimensional (with 10-100 state variables) complicated dynamic model is obtained that is unnecessarily complex for control applications.

There are a few papers in the literature that report on developing simple dynamic models for boiling water or pressurized water reactors for various purposes. A simple model was developed by [15] for the thermal-hydraulics part of a BWR reactor that is used for stability analysis of the reactor under different operating conditions. A relatively simple dynamic model used in a training course for simulation purposes is reported in [25]. There are also a few simple dynamic models available for the individual operating units in the primary circuit. A similar approach to ours has been used for the modeling and identification of a drum boiler in a boiling water reactor in [2]. Simplified models of the primary circuit dynamics of VVER plants were published in [39, 40] where the pressurizer model as a subsystem is included with slightly different assumptions from what are used in this paper.

Based on the above considerations, a simplified lumped dynamic model of the pressurizer in original physical coordinates is presented in this section for identification and control design purposes. The applied method is to use first engineering principles to capture the most important dynamics of the system [9].

## *2.2. System description and operation*

The VVER is a pressurized water reactor, that keeps the pressure of the primary circuit high enough such that the coolant cannot boil. The task of the pressurizer is to keep this pressure within a predefined range. The pressurizer is a vertical tank within which there is hot water at a temperature of about 325°C and steam above. If the primary circuit pressure decreases, electric heaters switch on automatically in the pressurizer. Due to the heating more steam will evaporate and this leads to a pressure increase. If the increasing pressure in the pressurizer reaches a certain limit, firstly the heaters are turned off and then cold water is injected into the tank (if needed) to reduce the pressure down to the predefined range [23]. The water injection is considered an emergency operation and therefore it will not be modeled. In the original configuration, four heater groups each having 90kW of power could be separately turned on/off and therefore it was not possible to keep the pressure in

a sufficiently narrow range. However, after the reconstruction, the heating power can be set continuously in the range of 0–360kW. This heating power expressed in units of 90kW is the system input ( $u$ ), and the measured and controlled output is the pressure in the tank (see Fig. 1).

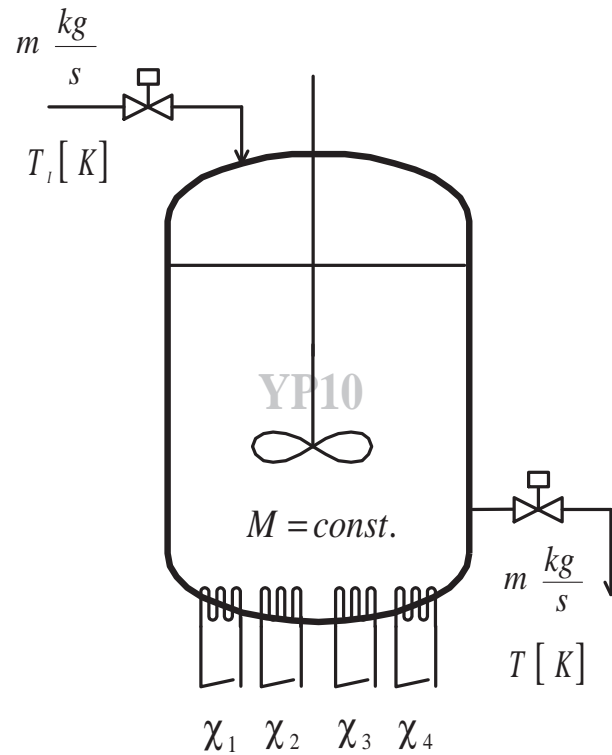


Figure 1: Simplified flowsheet of the pressurizer

### 2.3. Engineering model

The intended use of the model is controller design in *normal operating mode where the vapor can be considered to be in equilibrium with the liquid phase (saturated vapor)*, i.e. the dynamics of the vapor phase is infinitely quick compared to the other dynamic effects and the mass of the vapour phase is negligible compared to the other masses. Therefore, we can assume that the pressurizer contains pure water (the boron content is negligible) that is in

equilibrium with the vapor. Furthermore, constant physico-chemical properties and constant overall mass are assumed for both the water and the wall of the tank. Thus, the simplified model consists of two *energy balances*: one for the water and another one for the wall of the tank as balance volumes.

*Water energy balance*

$$\frac{dU}{dt} = c_p m T_I - c_p m T + K_W (T_W - T) + W_{HE} \cdot u \quad (1)$$

*Wall energy balance*

$$\frac{dU_W}{dt} = K_W (T - T_W) - W_{loss} \quad (2)$$

The following *constitutive equations*, describing the relationship between the internal energies and the corresponding temperatures, complete the model.

$$U = c_p M T, \quad (3)$$

$$U_W = C_{pW} T_W, \quad (4)$$

The variables and parameters of the above model and their units of measure are shown in Table 1.

We can list the disturbances with physical meaning as follows.

- *Primary circuit water infiltration*

This effect is taken into account with the in-convection term  $c_p m T_I$  in the water energy conservation balance (1), where the in- and outlet mass flowrate  $m$  is controlled to be equal (but might change in time) and the inlet temperature  $T_I$  can also be time-varying.

- *Energy loss*

This effect is modeled as a loss term  $W_{loss}$  in the wall energy balance (2).

The pressure of saturated vapor in the gas phase of the tank depends strongly on the water temperature in a nonlinear (exponential) way. The experimental measured data found in the literature [24] have been used to create an approximate analytic function to describe the dependence. The function has the form

$$p = h(T) = \frac{e^{\varphi(T)}}{100}, \quad (5)$$

Table 1: Model variables and parameters

$T$	water temperature	$^{\circ}\text{C}$
$T_W$	tank wall temperature	$^{\circ}\text{C}$
$c_p$	specific heat of water	$\frac{\text{J}}{\text{kg}^{\circ}\text{C}}$
$U$	internal energy of water	J
$U_W$	internal energy of the wall	J
$m$	mass flow rate of water	$\frac{\text{kg}}{\text{s}}$
$T_I$	inlet water temperature	$^{\circ}\text{C}$
$M$	mass of water	kg
$C_{pW}$	heat capacity of the wall	$\frac{\text{J}}{^{\circ}\text{C}}$
$u$	input heating power	90kW
$K_W$	wall heat transfer coefficient	$\frac{\text{W}}{^{\circ}\text{C}}$
$\chi_i$	on/off (1/0) state of the $i^{\text{th}}$ heater	–
$W_{loss}$	heat loss of the system	W

where  $\varphi(T) = c_0 + c_1T + c_2T^2 + c_3T^3$ . For the parameters of  $\varphi$ , the following values were obtained

$$c_0 = 6.5358 \cdot 10^{-1}, \quad c_1 = 4.8902 \cdot 10^{-2}, \quad c_2 = -9.2658 \cdot 10^{-5}, \quad c_3 = 7.6835 \cdot 10^{-8} \quad (6)$$

The validity range of the model is the usual operating domain of the pressurizer, i.e.  $315^{\circ}\text{C} \leq T \leq 350^{\circ}\text{C}$ . In pressure terms, this means  $105.65 \text{ bar} \leq p \leq 137.09 \text{ bar}$ .

#### 2.4. Continuous time state-space model

Based on eqs (1)-(2) and (3)-(4) we can write the system model in the following standard state-space form

$$\dot{x} = Ax + Bu + Ed \quad (7)$$

where the state vector  $x = [T \ T_W]^T$ , the manipulable input  $u \in [0, 4]$ . The disturbance input vector is  $d = [T_I \ W_{loss}]^T$ . Additionally, the matrices in (7) are the following

$$A = \begin{bmatrix} -\frac{m}{M} - \frac{K_W}{c_p M} & \frac{K_W}{c_p M} \\ \frac{K_W}{C_{pW}} & -\frac{K_W}{C_{pW}} \end{bmatrix}, \quad B = \begin{bmatrix} \frac{W_{HE}}{c_p M} \\ 0 \end{bmatrix}, \quad E = \begin{bmatrix} \frac{m}{M} & 0 \\ 0 & -\frac{1}{C_{pW}} \end{bmatrix}, \quad (8)$$

The physically measurable output of the system is the pressure  $p$  in the pressurizer but we assume that the function  $h$  in Eq. (5) is known and invertible, therefore we can write a linear output equation

$$y = \begin{bmatrix} 1 & 0 \end{bmatrix} x \quad (9)$$

with  $x_1 = h^{-1}(p)$ .

### 3. Model identification

#### 3.1. Structure estimation

To validate the proposed model structure (8), a particularly useful tool is the elementary subsystem (ESS) representation of the discrete time transfer function of the system. The ESS structure estimation algorithm proposed by [16] and the recursive estimation algorithm [5] is started from an overestimated structure and its parameters. By using a prediction error method, a maximum likelihood estimator finds the smallest required model structure and its parameters. Because of the advantageous parametrization, the method has excellent convergence properties. In the case of output error estimation, the method works with the following set of discrete-time models:

$$y(k) = \sum_{i=1}^{n_r} \frac{b_i z^{-1}}{1 + a_i z^{-1}} u(k-d) + \sum_{i=1}^{n_c} \frac{q_{1i} z^{-1} + q_{2i} z^{-2}}{1 + p_{1i} z^{-1} + p_{2i} z^{-2}} u(k-d) \quad (10)$$

where the required structural parameters are  $n_r$  and  $n_c$  for the number of real poles and complex pole-pairs respectively,  $d$  for the time delay. The model parameters are  $a_i$ ,  $b_i$ ,  $q_{ij}$  and  $p_{ij}$ .

In our case, the basic question at this step was the following: Based on the measured input-output data, is it worth dividing our system model into more balance volumes than it is written in Eqs. (1)-(2), i.e. is a more detailed lumped system model able to reproduce

the measured output in a better way? The results showed that already one real pole can describe the input-output behavior of the system in a satisfactory way, and two real poles bring only limited improvement compared to this. Involvement of complex pole-pairs and any additional real poles do not improve the prediction error at all. This means that the effective identification of the structure (8)-(8) is possible only if we can separate the dynamics of the water and the tank wall temperature by using some prior engineering information. Luckily, the knowledge of the water mass  $M$  gave us this necessary information (see section 3.3). More details about the structure estimation can be found in [31].

### 3.2. Structural identifiability analysis

Once the model structure is fixed, the next key step is parameter estimation the quality of which is crucial in the later usability of the obtained model [17]. It is known however, that physical parametrization is often not the best one for system identification from a computational point of view and alternative parametrizations have to be found e.g. to obtain a convex objective function in the transformed parameters [19], [18]. The notations and methods used in this section are taken from [19] where the necessary additional details can be found.

The model class considered is of the following form

$$\dot{x} = f(x, u, \theta), \quad x(0) = x_0 \quad (11)$$

$$y = h(x, u, \theta) \quad (12)$$

where  $x \in \mathbb{R}^n$  is the state vector,  $y \in \mathbb{R}^m$  is the output,  $u \in \mathbb{R}^k$  is the input, and  $\theta \in \mathbb{R}^d$  denotes the parameter vector. We assume that the functions  $f$  and  $h$  are polynomial in the variables  $x, u$  and  $\theta$ .

Shortly speaking, global structural identifiability means that

$$\hat{y}(t|\theta') \equiv \hat{y}(t|\theta'') \Rightarrow \theta' = \theta'' \quad (13)$$

where

$$\hat{y}(t|\theta) = h(x(t, \theta), u(t), \theta) \quad (14)$$

and  $x(t, \theta)$  denotes the solution of (11) with parameter vector  $\theta$ .

The structure (11) is globally identifiable if and only if by differentiating, adding, scaling and multiplying the equations the model can be rearranged to the parameter-by-parameter linear regression form:

$$P_i(u, y; p)\theta_i - Q_i(u, y; p) = 0 \quad i = 1, \dots, d \quad (15)$$

where  $P_i(u, y; p)$  and  $Q_i(u, y; p)$  are *differential polynomials* in  $u$  and  $y$ , and  $p$  denotes time differentiation.

The environmental energy loss  $W_{loss}$  is a non-measurable disturbance and it will be treated as constant. Let us introduce the following transformed parameters for Eqs. (7)-(8)

$$p_1 = \frac{m}{M}, \quad p_2 = \frac{K_W}{c_p M}, \quad p_3 = \frac{1}{c_p M}, \quad p_4 = \frac{K_W}{C_{pW}}, \quad p_5 = -\frac{1}{C_{pW}} W_{loss} \quad (16)$$

Then the system model can be written as

$$\dot{x}_1 = (-p_1 - p_2)x_1 + p_2 x_2 + p_1 d_1 + p_3 u, \quad (17)$$

$$\dot{x}_2 = p_4 x_1 - p_4 x_2 + p_5 \quad (18)$$

$$y = x_1 \quad (19)$$

After eliminating  $x_1$ ,  $x_2$  and using the fact that  $T_I$  was known and constant during the observed operation, we obtain the following input-output relation:

$$\ddot{y} = (-p_1 - p_2 - p_4)\dot{y} + p_1 p_4 (d_1 - y) + p_3 p_4 u + p_2 p_5 + p_3 \dot{u} \quad (20)$$

It is easy to see that (20) is in a standard regression form where the further transformed parameter vector  $\theta$  is given by

$$\theta = \left[ \begin{array}{ccccc} (-p_1 - p_2 - p_4) & p_1 p_4 & p_3 p_4 & p_2 p_5 & p_3 \end{array} \right]^T \quad (21)$$

It is also visible that by taking the further time derivatives of (20) and expressing and substituting  $\theta_i$ s, the parameter-by-parameter regression form (15) can be obtained (although the expressions for  $P_i$  and  $Q_i$  become quite lengthy during the calculations).

If we have an estimation for  $\theta$ , then  $p_1, \dots, p_5$  can be computed in the following order:

$$p_3 = \theta_5, \quad p_4 = \theta_3/p_3, \quad p_1 = \theta_2/p_4, \quad p_2 = -\theta_1 - p_1 - p_4, \quad p_5 = \theta_4/p_2 \quad (22)$$

The above computations show that the model (18)-(19) is *structurally identifiable* with parameters  $p_1, \dots, p_5$  if the disturbance  $T_I$  is constant.

There are altogether six physical parameters in the equations (16), namely:  $m$ ,  $M$ ,  $c_p$ ,  $K_W$ ,  $C_{pW}$ , and  $W_{loss}$ . Naturally, all these six parameters cannot be separately identified from  $p_1, \dots, p_5$  and we have to rely on some prior knowledge to be able to determine them.

A realistic approach is that the measured constant flow rate  $m$  is assumed to be known. In this case, the physical parameters can be determined as follows

$$M = \frac{m}{p_1}, \quad c_p = \frac{1}{Mp_3}, \quad K_W = p_2 c_p M, \quad C_{pW} = \frac{K_W}{p_4}, \quad W_{loss} = -p_5 C_{pW} \quad (23)$$

From the above results we can conclude that the model is structurally identifiable also in the physical coordinates if  $m$  is known a-priori. The detailed computations for this can be found in [28].

### 3.3. Model parameter estimation

For the model parameter estimation, a pressure measurement record of about 10 hours were used with a sampling time of 10s. The input of the system consisted of 5 switchings between two discrete values of the manipulable input, where the switching times were exactly known. It is important to note that the constraints of the industrial environment seriously limited the type of applicable input signals.

The temperature-pressure curve was inverted by evaluating (5) at 200 equidistant points between 315 °C and 350 °C and approximating the inverse using 3<sup>rd</sup> order splines. The measured input and output of the system is shown in Fig. 2.

The objective function to be minimized was the standard squared two-norm of the difference between the measured and simulated output, i.e.

$$V_T = \int_0^T \epsilon^2(t, \theta) dt \quad (24)$$

where  $\epsilon(t, \theta) = y(t) - \hat{y}(t|\theta)$  and  $y$  denotes the measured temperature data. The obtained physical parameter values were the following (their units of measure are found in Table 1):

$$m = 0.15, \quad M = 30138, \quad K_W = 63204, \quad c_p = 4183, \quad C_{pW} = 4.8477 \cdot 10^7, \quad W_{loss} = 1.3588 \cdot 10^5 \quad (25)$$

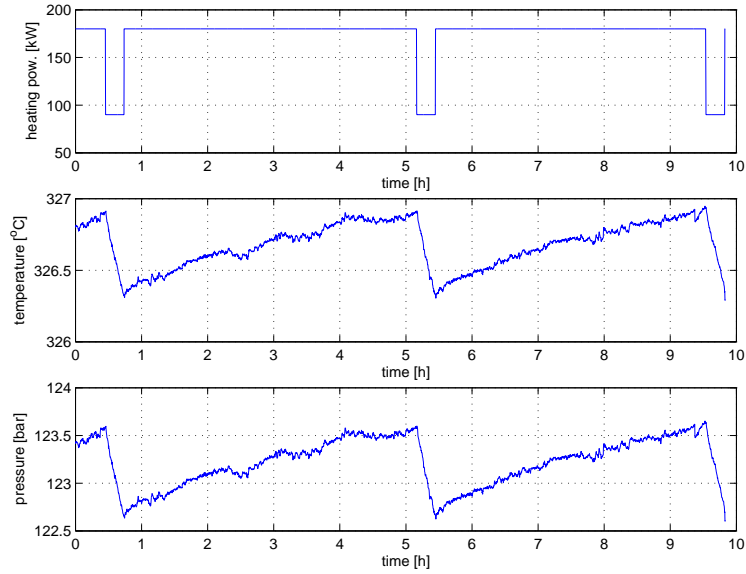


Figure 2: Measured input and output of the system

The objective function value with the above parameters was  $V_T = 26.31$ . The orders of magnitude and values of the estimated parameters are fully acceptable from a physical point of view. The fit between the measured and simulated temperatures is fairly good as it is visible in Fig. 3. It can also be seen on the small variations of the measured temperature that some unmodeled phenomena (e.g. evaporation and precipitation) took place in the system or certain parameters were actually not constant during the operation.

## 4. The controller design method

### 4.1. Dynamic inversion-based control design

Recently, controller design based on dynamic inversion has gained considerable interest, particularly in the field of aerial and space vehicles [13], [21].

In order to design an advanced controller for the pressurizer, the reference tracking problem of a Wiener system, i.e. an interconnection of an LTI system with a static output nonlinearity, has to be solved. The problem of (asymptotic) tracking consists in finding

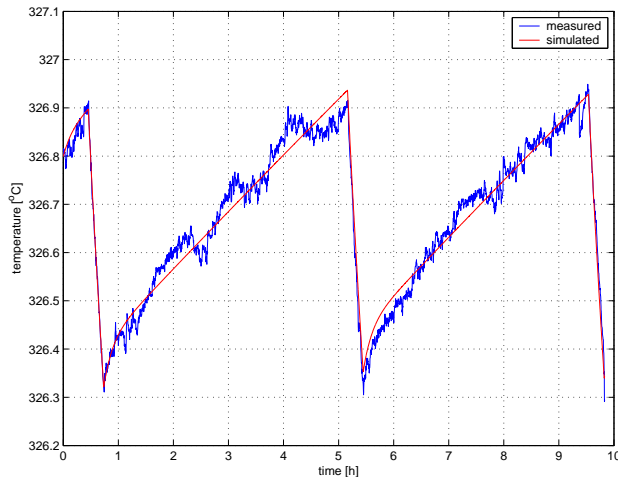


Figure 3: Fit between measured and simulated temperatures

a compensator such that the closed-loop system is internally stable and for any desired trajectory  $y_d$  the output of the closed-loop system (asymptotically) approaches  $y_d$ .

There are numerous papers dealing with the control design based on Wiener model structure, e.g. [14], [33], [37]. Usually, for controller design purposes the static non-linearities are removed by an inversion, however, the inverse of the nonlinearity can be delivered by the identification algorithm, too. The special way in which the nonlinearity enters the Wiener model can be exploited by transforming it into uncertainty. The result will be an uncertain linear model, which enables to use for example robust linear MPC techniques, see [4], [36].

Different type of problems can be distinguished based on the structure imposed to the set of the desired trajectories. The most highly structured situation is when this set is finite [10]. If the class of desired trajectories can be described by an exosystem, i.e., an autonomous, noninitialized set of differential equations with an output, then the problem is called the regulator or servomechanism problem [11]. If  $y_d$  is generated by a model that is a forced, noninitialized dynamical system, the problem is usually termed as (asymptotic)model matching [6], [12].

In this section the design of the dynamic inverse of the linear part of the Wiener model will be presented following [27] where more details can be found. The unmeasured output  $z$  it is supposed to be computed using a static nonlinear inverse function that it is assumed to

be given. In most of the cases, this static inverse function is provided by an identification process of a Wiener model as a spline approximation, or by an approximation given by a suitable set of orthonormal functions, e.g. Chebysev polynomials or wavelets. By this assumption, instead of the desired output  $y_d$  of the nonlinear system, one can also work with the corresponding desired output of the linear part of the system, i.e.  $z_d$ .

Let us recall that if the system is invertible, then  $V^*$ , i.e. the maximal (A,B)-invariant subspace contained in  $\ker C$ , induces a decomposition of the linear system into:

$$\dot{x}_1 = A_{11}x_1 + A_{12}x_2 + B_1u \quad (26)$$

$$\dot{x}_2 = A_{21}x_1 + A_{22}x_2 \quad (27)$$

$$z = C_1x_1, \quad (28)$$

where  $\text{Im}B = \text{Im}B_1$  and  $x_1 \in V^{*\perp}$ , see [3], [38]. Let us denote the subsystem formed by (26) and (28) by  $\Sigma_1$  and the subsystem (27) by  $\Sigma_2$ .

By applying the feedback  $u = F_1x_1 + F_2x_2 + v$ , with  $F = [F_1 \ F_2]^T$  that renders  $V^*$   $(A + BF, B)$  invariant, one can obtain the system:

$$\dot{x}_1 = A_{11}x_1 + B_1v, \quad z = C_1x_1. \quad (29)$$

Let us denote this system by  $\Sigma_{1,f}$ . By choosing a solution  $F_2$  of the equation  $A_{12} + B_1F_2 = 0$  one can set  $F_1 = 0$ .

Denoting by  $c_i$  the rows of  $C_1$  let us consider the subspace

$$\text{span}\{c_1, \dots, c_1A_{11}^{\gamma_1}, \dots, c_p, \dots, c_pA_{11}^{\gamma_p}\} \quad (30)$$

where  $c_lA_{11}^lB_1 = 0$ , for  $l < \gamma_l$ , and  $\gamma_l$  are chosen such that the spanning vectors are linearly independent. It follows, that choosing the basis (30) for  $V^{*\perp}$ , one can define a coordinate transform  $\mathcal{S}$  that maps  $x_1$  to  $\tilde{z}$ , where

$$\tilde{z} = \left[ z_1, \dots, z_1^{(\gamma_1)}, \dots, z_p, \dots, z_p^{(\gamma_p)} \right]^T. \quad (31)$$

In this basis one has a particular simple form of the decomposition (29). It follows, that

$$v = B_1^{-r}S^{-1}(\dot{\tilde{z}} - SA_{11}S^{-1}\tilde{z}) := \lambda(z), \quad (32)$$

$$x_1 = S^{-1}\tilde{z} := \zeta(z), \quad (33)$$

where  $B_1^{-r}$  is the right inverse of  $B_1$ .

The required input to track a desired output signal  $z_d$  is given by the dynamic system

$$\dot{\eta}_d = A_{22}\eta_d + A_{21}\zeta(z_d) \quad (34)$$

$$u_d = F_2\eta_d + \lambda(z_d), \quad (35)$$

provided that this input is applied to the original system started from the initial condition given by  $x_0 = T^{-1} \begin{bmatrix} x_{10} \\ x_{20} \end{bmatrix}$ , where  $x_{20}$  can be arbitrarily chosen but  $x_{10}$  should be set to  $x_{10} = S^{-1}\tilde{z}_d(0)$ .

In practice it seldom happens that one can impose on the system the required initial conditions, therefore, there will be an error in the whole state. To close the loop, a suitable linear dynamical system of the tracking error is added to the linearizing control input. By examining the "open-loop" equations (34) one can observe that it is possible to introduce an "outer-loop" by applying an error feedback, that modifies the equations (35) that define the control input. This idea is highlighted by the dotted line part of Figure 4.

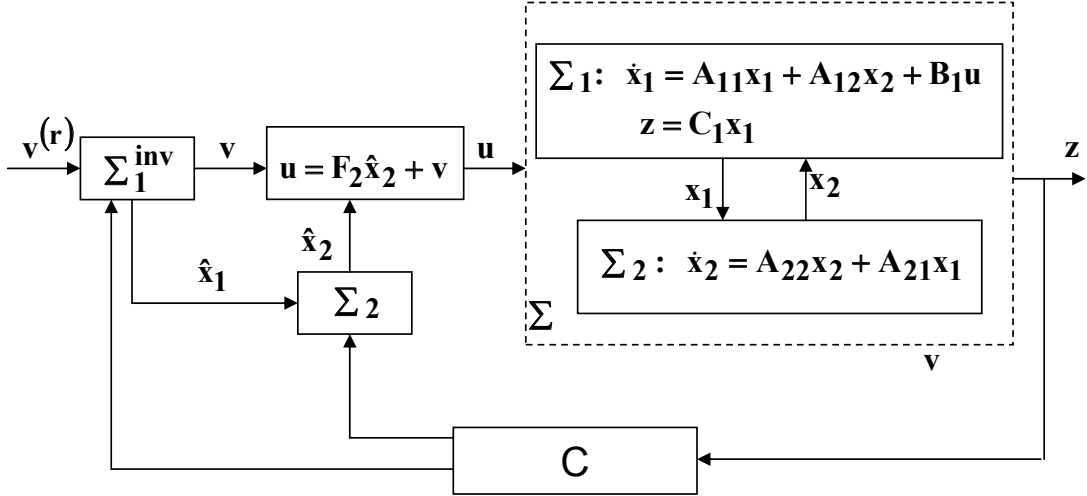


Figure 4: Inversion based tracking

Based on this structure, an advanced (e.g.  $\mathcal{H}_\infty$ ) controller can be designed in order to minimize the influence of the disturbances on the performance of the tracking error.

**Remark 1.** *In order to cope with the problem of disturbances and measurement noise it is suitable to have additional measurements, that makes the pair  $(A + BF, \bar{C})$  fully observable. In this case the designer has additional possibilities to set a meaningful  $\mathcal{H}_\infty$  control problem, and to guarantee robust performance properties of the controller.*

**Remark 2.** *The dynamic inverse system for discrete systems can be obtained in a similar manner by using the shift operator  $qu(t) = u(t + 1)$  instead of the differentiation operator. The derivation is straightforward, hence it is omitted.*

#### 4.2. Controller design for the pressurizer

The main control goal is to stabilize the pressure at a prescribed reference value (typically around 123-124 bars which is equivalent to approximately 327 °C in terms of temperature). Moreover, the controller's additional task is to suppress the effect of measurement noise and that of the time-varying disturbances  $(W_l, T_I)$ .

Using the theory described in section 4.1, the brief summary of the controller design method is the following. The state-space equations of the open loop system (7) can be rewritten as

$$\dot{x}_1 = a_{11}x_1 + a_{12}x_2 + B_u u + E_T T_I \quad (36)$$

$$\dot{x}_2 = a_{21}x_1 + a_{22}x_2 - E_W W_l \quad (37)$$

where  $a_{ij} = A_{ij}$ ,  $B_u = B_1$ ,  $E_T = E_{11}$  and  $E_W = E_{22}$  in (8)-(8). Let  $x_1^r$  denote the reference value for  $x_1$  (i.e.  $z_d = x_1^r$ ). Furthermore, let us denote the nominal (mean) values for the time-varying disturbances by  $T_{I,n}$  and  $W_{l,n}$ , respectively.

Note that the system equations (36)-(37) are already in the form of eqs. (26)-(27) with extra disturbance terms. Since  $A_{11} = a_{11}$  is a scalar, we don't need the general coordinates transformation  $\mathcal{S}$  described in section 4.1, and the equations of the inversion controller can be derived in the following straightforward way. The dynamic equation of the inversion controller is given by

$$\dot{\eta} = a_{22}\eta + a_{21}x_1^r - E_W W_{l,n} \quad (38)$$

The input  $u$  is expressed as  $u = u^r + v$ , where

$$u^r = \frac{1}{B_u}(\dot{x}_1^r - a_{11}x_1^r - a_{12}\eta - E_T T_{I,n}), \quad (39)$$

and  $v$  is a new input term for additional feedback.

The state variables of the tracking error system are defined as

$$s_1 = x_1 - x_1^r, \quad s_2 = x_2 - \eta \quad (40)$$

Substituting (39) into (36) gives

$$\dot{x}_1 = a_{11}(x_1 - x_1^r) + a_{12}(x_2 - \eta) + E_T \tilde{d}_1 \quad (41)$$

where  $\tilde{d}_1 = T_I - T_{I,n}$ . For the tracking error dynamics, we get

$$\dot{s}_1 = a_{11}s_1 + a_{12}s_2 + E_T \tilde{d}_1 + B_u v \quad (42)$$

$$\dot{s}_2 = a_{21}s_1 + a_{22}s_2 - E_W \tilde{d}_2 \quad (43)$$

where  $\tilde{d}_2 = W_l - W_{l,n}$ .

Taking into consideration that  $x_1$  is the measured state variable, we can shape the error dynamics with a dynamic (or static) controller of the general form

$$\dot{\xi} = M_{c1}\xi + M_{c2}s_1 \quad (44)$$

$$v = M_{c3}\xi + M_{c4}s_1, \quad (45)$$

#### 4.3. Simulation tests

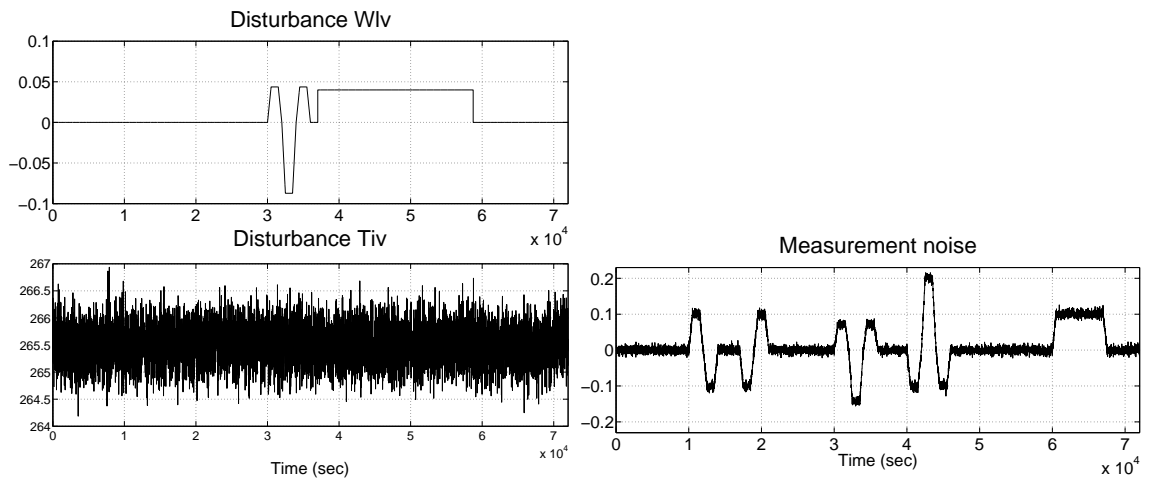
The conditions of the simulation were the following: there were applied noisy  $W_{loss}$  and noisy  $T^i$  and it was considered also a disturbance. These are shown in Figure 5(a) and 5(b).

The signal given by the controller is illustrated in Figure 5(c). Due to the physical restrictions imposed by the actuator the actual control input differs slightly from the required one.

The simulated output of the linear part of the system (temperature) is shown in Figure 5(d). The computed values based on the measurements  $T_p$  and the noise free outputs  $T$  are also depicted.

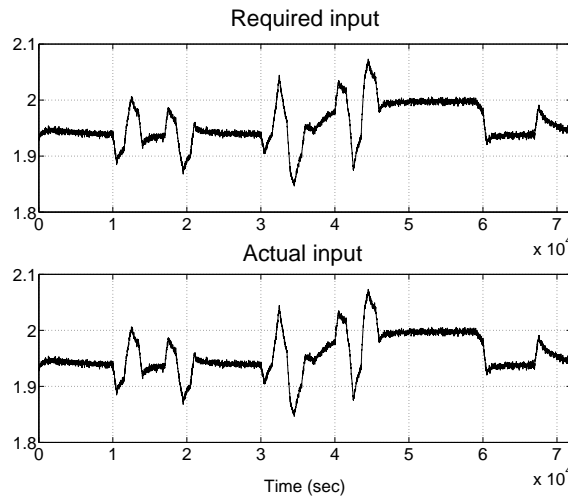
The simulated output of the nonlinear system (pressure) is shown in Figure 5(e). The noise free computed values  $p$  and the measured values  $p_z$  are also illustrated.

The regulated values of the pressure remained between the specified required levels, i.e., between 123.5 and 124 bar.

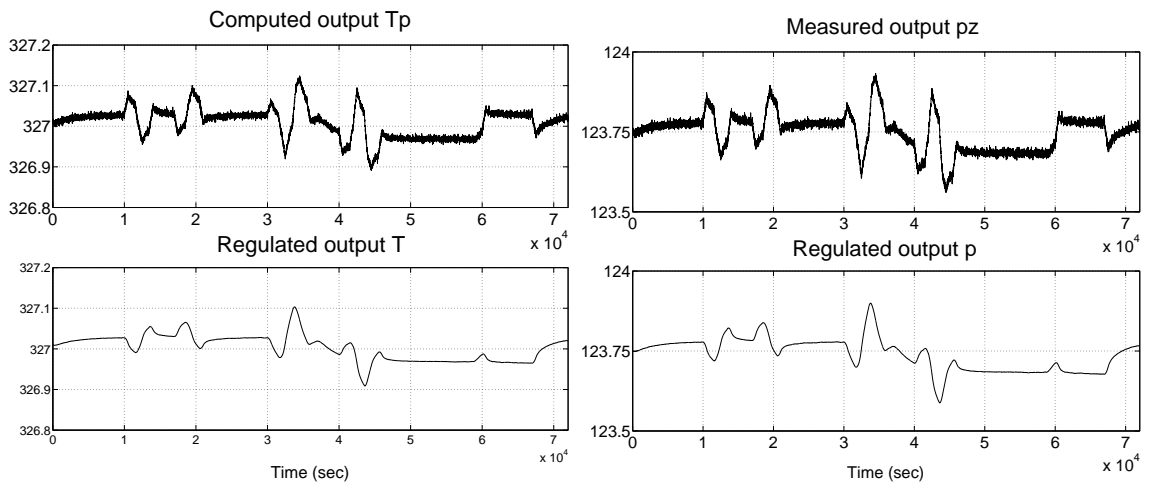


(a) Disturbances applied in the simulation

(b) Noise applied in the simulation



(c) The control input



(d) The output of the linear part of the system: temperature (e) The output of the nonlinear system: pressure

Figure 5: Result of a simulation analysis

## 5. Performance analysis of the networked control solution

### 5.1. Theoretical background

It is well known that the performance or even the stability of a networked control loop are significantly influenced by network phenomena such as delays, packet losses or link failures [30], [32]. The concepts and results summarized in this subsection are mostly taken from [22] and [30]. The basic configuration of a networked control system can be seen in Fig. 6, where  $x_p$  and  $x_c$  are the states of the plant and the controller, respectively,  $y \in \mathbb{R}^r$  is the plant output,  $u \in \mathbb{R}^p$  is the controller output, while  $\hat{y} \in \mathbb{R}^r$  and  $\hat{u} \in \mathbb{R}^p$  are the most recently transmitted plant and controller output values through the network.  $e$  is the error caused by network transmission that is defined as

$$e(t) = \begin{bmatrix} \hat{y}(t) - y(t) \\ \hat{u}(t) - u(t) \end{bmatrix} \quad (46)$$

Individual actuators and sensors connected to the networks are called nodes. We assume that node data are transmitted at time instants  $\{t_0, t_1, \dots, t_i\}$  where  $i \in \mathbb{N}$ . The transmission time instants satisfy  $\epsilon < t_{j+1} - t_j \leq \tau$  for  $j \geq 0$  where  $\epsilon, \tau > 0$ . The upper interval bound  $\tau$  is called the *maximum allowable transfer interval* (MATI).

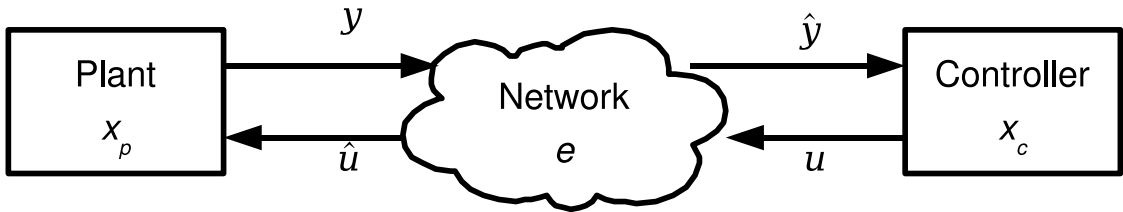


Figure 6: Networked control system

Using the notation  $x = [x_p^T \ x_c^T]^T \in \mathbb{R}^n$ , the dynamic equations of a networked control system with disturbance vector  $w \in \mathbb{R}^m$  between the transmission instants can be written as

$$\dot{x} = f(t, x, e, w), \quad t \in [t_{i-1}, t_i] \quad (47)$$

$$\dot{e} = g(t, x, e, w), \quad t \in [t_{i-1}, t_i] \quad (48)$$

The discontinuous change of  $e$  during transmission instants can be modeled as a jump system

$$e(t_i^+) = (I - \Psi(i, \hat{e}(t_i)))e(t_i) \quad (49)$$

$$\hat{e}(t_i^+) = \Lambda(i, \Psi(i, \hat{e}(t_i))e(t_i), \hat{e}(t_i)) \quad (50)$$

where  $\hat{e}$  is the decision vector of the network scheduler,  $\Psi$  is the scheduling function and  $\Lambda$  is the decision update function. More details about the dynamics (49)-(50) in the case of different scheduling protocols can be found in [30]. A key feature of network scheduling protocols from the point of view of closed loop stability is the so-called *persistently exciting* (PE) property. According to the definition, a protocol is *uniformly PE in time  $T$*  if it regularly visits every network node within a fixed period of time  $T$ .

In the LTI or linearized case Eqs. (47)-(48) will be used in the form

$$\dot{x} = \Phi_{11}x + \Phi_{12}e \quad (51)$$

$$\dot{e} = \Phi_{21}x + \Phi_{22}e \quad (52)$$

where  $\Phi_{ij}$  are constant matrices of appropriate dimensions.

Let us introduce the following notations.  $\mathcal{A}_n^+$  denotes the set of positive semidefinite symmetric  $n \times n$  matrices with positive entries. For  $x, y \in \mathbb{R}^n$ ,  $x \preceq y \iff x_i \leq y_i$  for  $i = 1, \dots, n$ . For an  $n$ -dimensional vector  $x$ ,  $\bar{x} = [|x_1|, \dots, |x_n|]^T$ . The following theorem from [30] will serve as a theoretical basis for our forthcoming calculations in section 5.2.

*Theorem 1:* Suppose that the NCS scheduling protocol of (47)-(50) is uniformly persistently exciting in time  $T$  and the following assumptions hold

1. There exist  $Q \in \mathcal{A}_n^+$  and a continuous output of the form  $\tilde{y}(x, w) = G(x) + w$  so that the error dynamics (48) satisfies

$$\bar{g}(t, x, e, w) \preceq Q\bar{e} + \tilde{y}(x, w) \quad (53)$$

for all  $(x, e, w)$ , for  $t \in (t_i, t_{i+1})$ , and for all  $i \in \mathbb{N}$ .

2. (47) is  $\mathcal{L}_p$  stable from  $(e, w)$  to  $G(x)$  with gain  $\gamma$  for some  $p \in [1, \infty]$ .
3. the MATI satisfies  $\tau \in (\epsilon, \tau^*)$ ,  $\epsilon \in (0, \tau^*)$ , where

$$\tau^* = \ln(v)/(|Q|T), \quad (54)$$

and  $v$  is the solution of

$$v(|Q| + \gamma T) - \gamma T v^{1-1/T} - 2|Q| = 0. \quad (55)$$

Then the NCS is  $\mathcal{L}_p$ -stable from  $w$  to  $(G(x), e)$  with linear gain.

Using Theorem 1, a sharp and practically usable estimation can be obtained for the acceptable upper bound of the MATI such that the  $\mathcal{L}_p$  stability of the closed loop system is preserved.

### 5.2. The controlled pressurizer as an NCS

For the simplification of the forthcoming calculations, we will use the following (sometimes simplifying) assumptions for the analysis.

- $\mathcal{A}1$  The time-varying disturbances  $T_I$  and  $W_l$  are constant. This assumption approximates reality quite well if we consider a few minutes to approximately one hour of system operation, because the change of these disturbances is usually rather slow compared to the system dynamics.
- $\mathcal{A}2$  The nominal values of disturbances  $(T_{I,n}, W_{l,n})$  are constant.
- $\mathcal{A}3$  Zero order hold is assumed on the input.
- $\mathcal{A}4$  The temperature reference  $x_1^r$  is (at least piecewise) constant.
- $\mathcal{A}5$  Pressure measurement noise is not taken into consideration during the analysis.
- $\mathcal{A}6$  Similarly to the examples in [30], all the network induced errors are grouped to the output, i.e.  $e = \hat{y}(t) - y(t)$ .

The analyzed dynamic inversion based controller uses a static error feedback, therefore the controller equations (38), (39) and (45) can be summarized in the following simple state-space model containing only one state variable (denoted by  $x_3$ ):

$$\begin{aligned} \dot{x}_3 &= A_c x_3 + B_{c1} x_1 + (B_{c1} - B_{c4}) x_1^r + B_{c3} W_{l,n} \\ y_c &= D_{c4} x_1 + C_c x_3 + (D_{c1} - D_{c4}) x_1^r + D_{c2} T_{I,n} \end{aligned}$$

where  $A_c$ ,  $B_{ci}$ ,  $C_c$  and  $D_{ci}$  are the controller parameters, and  $x_1$  is the temperature in the pressurizer. The actual system input can be computed as

$$u = y_c + e \quad (56)$$

Using (56), the equations of the closed loop system can be written as

$$\begin{aligned} \dot{x}_1 &= (a_{11} + B_u D_{c4})x_1 + a_{12}x_2 + B_u C_c x_3 + E_T T_I \\ &\quad + B_u (D_{c1} - D_{c4})x_1^r + B_u D_{c2} T_{I,n} + B_u e \end{aligned} \quad (57)$$

$$\dot{x}_2 = a_{21}x_1 + a_{22}x_2 + E_W W_l \quad (58)$$

$$\dot{x}_3 = B_{c4}x_1 + A_c x_3 + (B_{c1} - B_{c4})x_1^r + B_{c3} T_{I,n} \quad (59)$$

$$y_c = D_{c4}x_1 + C_c x_3 + (D_{c1} - D_{c4})x_1^r + D_{c2} T_{I,n} \quad (60)$$

Observe, that we have a LTI closed loop system model. Therefore, from Eqs. (57)-(59), matrices  $\Phi_{11}$  and  $\Phi_{12}$  in (51) are obtained as

$$\Phi_{11} = \begin{bmatrix} a_{11} + B_u D_{c4} & a_{12} & B_u C_c \\ a_{21} & a_{22} & 0 \\ B_{c4} & 0 & A_c \end{bmatrix}, \quad (61)$$

$$\Phi_{12} = \begin{bmatrix} B_u \\ 0 \\ 0 \end{bmatrix} \quad (62)$$

Let us denote the  $i$ th row of  $\Phi_{11}$  by  $\Phi_{11}^i$ . Using assumptions  $\mathcal{A}1$ – $\mathcal{A}4$ , the time derivative of  $e$  can be written as

$$\begin{aligned} \dot{e} &= -\dot{y}_c = -D_{c4}\dot{x}_1 - C_c\dot{x}_3 = \\ &= -D_{c4}\Phi_{11}^1 x - C_c\Phi_{11}^3 x - D_{c4}B_u e - D_{c4}E_T T_I - D_{c4}B_u(D_{c1} - D_{c4})x_1^r - \\ &= D_{c4}B_u D_{c2} T_{I,n} - C_c(B_{c1} - B_{c4})x_1^r - C_c B_{c3} W_{l,n} \end{aligned} \quad (63)$$

From (63), matrices  $\Phi_{21}$  and  $\Phi_{22}$  of (52) are the following

$$\Phi_{21} = -D_{c4}\Phi_{11}^1 - C_c\Phi_{11}^3 \quad (64)$$

$$\Phi_{22} = -D_{c4}B_u \quad (65)$$

The controller parameters were the following

$$\begin{aligned}
A_c &= -0.0029, \quad B_{c1} = 0.0029, \quad B_{c3} = -0.0020, \\
B_{c4} &= 0.011, \quad C_c = -2.1031, \quad D_{c1} = 2.11, \\
B_{c2} &= -0.007, \quad B_{c4} = -7.58
\end{aligned} \tag{66}$$

Using the model of the closed loop system (57)-(60), the estimated model parameters (25) and the controller parameters (66), the matrices  $\Phi_{11}$ ,  $\Phi_{12}$ ,  $\Phi_{21}$  and  $\Phi_{22}$  are easy to compute (see [29] for the details).

Since the system is SISO, the number of network links can chosen to be one, i.e.  $T = 1$ .

The  $\mathcal{L}_2$  gain between the error  $e$  and the output  $\tilde{y} = \Phi_{21}x$  is  $\gamma = 9.595 \cdot 10^{-3}$ . For the estimation of  $\tau^*$ , first we solve Eq. (55) that yields  $z = 1.499$ . The norm of  $\Phi_{22}$  is easy to compute and thus:  $|\Phi_{22}| = |Q| = 9.5902 \cdot 10^{-3}$ .

From these results and by solving (55), we obtain the following estimate for the MATI:  $\tau^* = 42.27$  s. This proves, that the present sampling time of 10 s is a safe value from the point of view of  $\mathcal{L}_2$  stability even if there are some network induced delays that do not violate  $\tau^*$ .

## 6. Controller implementation

### 6.1. Safety and fault tolerance considerations

The implementation of the primary circuit control loops in nuclear power plants is a rather complex task. The safety requirements have very high priority during the design and construction of such systems. On the other hand, the continuity of the operation must be maintained and certain production criteria should be met at the same time.

It is widely accepted that it is advantageous to solve control problems in high complexity systems using a decentralized, hierarchical structure. Thus, modern controller implementations are often based on decentralized and embedded computer systems. A key part of the decentralized system is the communication media between the individual subsystems. In order to increase safety, it's essential that the control system contains redundancy. Redundancy in itself can be quite effective in handling certain faults, but there exist reconfigurable fault tolerant solutions that represent a higher degree of safety. If a fault occurs in such systems, the redundant elements are re-grouped following a centralized or decentralized scheme,

and the whole system can continue its operation in a more or less degraded way. Depending on the degree of degradation, one can decide for the continued operation (possibly with a parallel repair), or for the shutdown of the plant. Using a reconfigurable redundant system, it is generally possible to safely handle more serious faults than the ones that are treatable by simple redundant solutions.

Based on the above considerations, the implemented control system is a partially reconfigurable redundant system that was designed and introduced on the 1st, 3rd and 4th units of the NPP during the 2004-2006 period.

### *6.2. Implementation details*

The measurement of the physical variables is taking place locally and the measurement includes some pre-processing, filtering and credibility test. The measurement results are transferred to the computer system in a compressed format via digital network communication. The operation of the actuators is local, too, based on the input signals that are also transmitted through a digital network. To increase reliability, the actuation is completed with a checkback, the result of which is returned to higher levels of the controller hierarchy through the network.

The actual control is realized using a computer system interconnected by a digital communication network. The key decision-making elements of the system are the PLCs X, Y and W (see Fig. 7). The computers form a hierarchical system where the communication is going in such a way that each level gets the amount of data that is necessary for its functions and transmits such data that are requested by the higher levels. Overall reliability is improved by adding some redundancy to the levels.

The structure of the pressure controller is shown in Fig. 7. Pressure sensors A, B and a Profibus DP pressure sensor measure the pressure in the pressurizer. The sampling time is 250 ms, the measurements are processed by PLCs S1 and S2 using an averaging filter. Since the physical place of the pressure measurement is not identical to the place to which the controlled pressure corresponds, the pressure difference resulting from the height difference should be taken into account (also in PLCs S1 and S2). In each sampling instant, both sensors send a pressure measurement through the Profibus DP network, but only one selected record will be processed. The selection primarily depends on the first correct measurement record and on the credibility of certain signals. The selection procedure runs in PLCs Y, X and

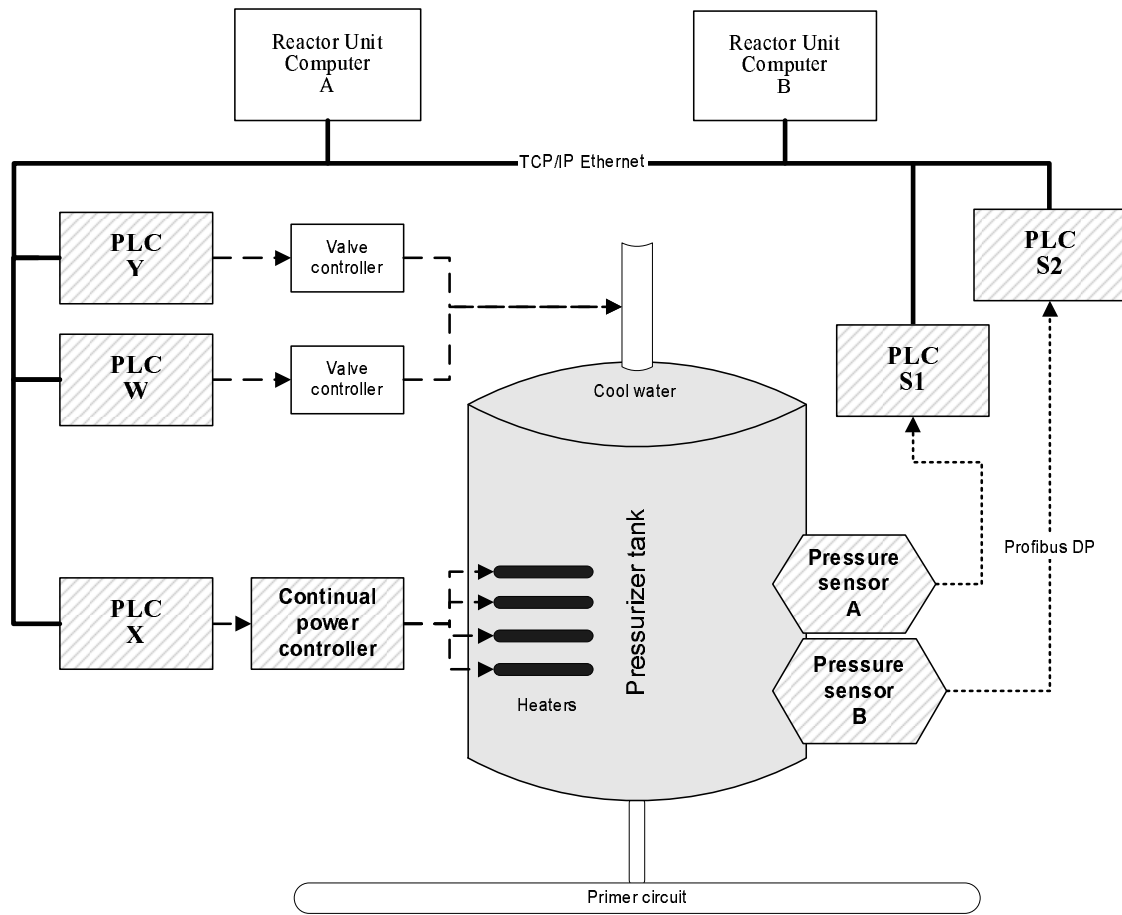


Figure 7: Structure of Reactor Pressure Controller System

W such that all three PLCs must select the same pressure value. This requires that the selection procedures to be implemented using majority (2v3) voting logic that must be free of any functional hazards. The main tasks of PLCs S1 and S2 are the pre-processing and transmission of pressure measurements towards PLC units Y, X and W. The other task of these units is the organization of communication between other units. The two PLCs control the transmission of messages in the network which means that each message reaches its target through these units.

The Y, X, and W PLCs contain the control algorithm and these devices drive the real

actuators. These fieldbus controllers are capable of supporting all I/O modules. The Y, X, W devices automatically configure themselves, creating a local process image which may include analog, digital or specialty modules. They are programmable according to IEC 61131-3 using 512 KB program memory, 128 KB data memory and 24 KB retentive memory. The 32-bit based CPU is capable of multitasking and has a battery backed real-time clock. The controller offers many different application protocols which can be used for data acquisition or control (MODBUS, ETHERNET /IP) or for system managing and diagnostics (HTTP, BootP, DHCP, DNS, SNTP, FTP, SNMP and SMTP). This fieldbus controller is suitable for data rates 100 Mbit/s via TCP/IP network. Protection against unauthorized access is also possible with full TCP /IP functionality. When the security option is switched on, only predefined clients can communicate with the controller.

An important part of the system is the power controller. This device is a solid state power controller with zero crossing switching for resistive loads with current ratings up to 600A and 660Vac nominal voltages. The controller accepts logical commands in volts, milliamperes or from a PLC. Using a trimmer, it is possible to set the cycle time which is used for the power modulation in relation to the input analogue signal. The control of the triphase loads can be made used as master and one or more controller extenders can be used as slaves. Each model is equipped with a logic input to disable the solid state relay/power controller and eventually break off power supply. Different options are available for the more critical applications, such as the load control which detects and indicates partial load failure interruption/cut-off, with a LED on the faceplate, and a relay alarm output.

The 'Reactor Unit Computer A and B' show the unit computers already existing in the unit, that connected to the pressure control system to display information about current conditions. There is an iFix SCADA system operating on these Unit Computers and they connected to the Y and W PLCs through a Modbus over TCP/IP protocol. They receive the information about the conditions of the pressure control system, which need to be displayed from these units.

### *6.3. Results and discussion*

The operational experiences of the new pressure controller are very good. Using the more efficient control, the pressure remains in a smaller interval than before. This made possible a safe increase in the thermal power of the units by 1-2%. The main feature of the

new controller is that a very stable pressure value is guaranteed compared to the previous oscillations, using a continuous range (0-360 kW) of heating power. The amplitude of the pressure oscillations was reduced from 1 bar to 0.1 bar, see Fig. 8. In this way, a much smoother overall operation has been obtained which is advantageous for the equipment in the primary circuit.

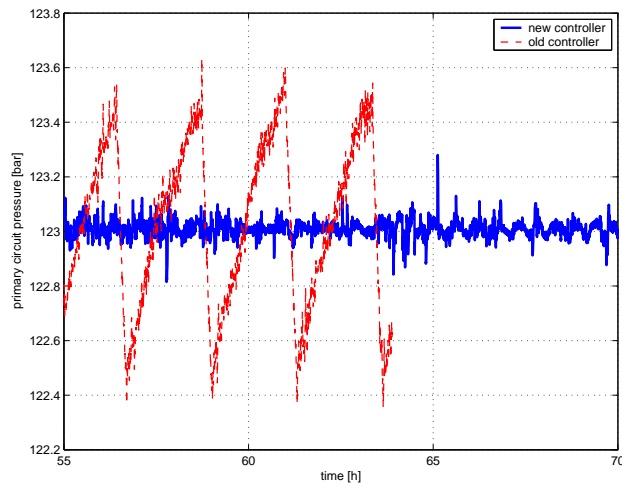


Figure 8: Pressure before and after the implementation of the new control scheme

## 7. Conclusion

The paper has presented the main steps of the design of a pressure controlling tank located in the primary circuit of the Paks Nuclear Power Plant in Hungary. Based on first engineering principles a Wiener model has been constructed which has been validated. Using the identification step a final model with known static nonlinearity is formulated.

For control design it is assumed that the inverse of the nonlinear part can be implemented. The proposed method does not assume that the full state vector is measured and it is based on a dynamic inversion approach with error feedback. The implemented controller has a hierarchically arranged distributed structure including measurement and control PLCs, a continuous power controller and a special supervisor module connected by a TCP/IP network.

Using the theory of networked control systems, the MATI has been computed which guarantees the  $\mathcal{L}_2$  stability properties of the closed loop system. The computed MATI value has been found much larger than the sampling time of the actually implemented networked controller. The calculations were checked against simulation results.

The hardware and software design and implementation obey the safety-critical requirements imposed by the special nature of the controlled plant by applying redundancy and special test operating modes and switching strategy for each system elements. The controller has been implemented and used in the units of Paks NPP. The use of the advanced controller resulted in a smooth overall operation, which is advantageous for the equipment in the primary circuit. In addition, it has been possible to safely increase the thermal power of the units by 1-2 %.

#### *Acknowledgement*

This work was supported by the Control Engineering Research Group of HAS at Budapest University of Technology and Economics. The support of the Hungarian Scientific Research Fund through grants T042710, F046223 is gratefully acknowledged. Gábor Szederkényi is the grantee of the Bolyai János Research Scholarship of the Hungarian Academy of Sciences. The authors gratefully acknowledge the continuous support of the members of the INC Refurbishment Project, especially the help of Tamás Túri, Béla Katics and Balázs Doszpod at the Paks Nuclear Power Plant.

- [1] APROS. APROS - the advanced process simulation environment, VTT industrial systems. 2005. <http://www.vtt.fi/tuo/63/apros/>.
- [2] K.J. Aström and R.D. Bell. Drum-boiler dynamics. *Automatica*, 36:363–378, 2000.
- [3] G. Basile and G. Marro. A new characterization of some structural properties of linear systems: unknown-input observability, invertability and functional controllability. *Int. J. Control*, 17:931–943, 1973.
- [4] H.H.J. Bloemen, T. J. J. van den Boom, and H.B. Verbruggen. Model-based predictive control for hammerstein-wiener systems. *International Journal of Control*, 74:482–495, 2001.

- [5] J. Bokor and L. Keviczky. Recursive structure, parameter and delay time estimation using ESS representations. pages 867–872, 1985.
- [6] M. D. di Benedetto and J.W. Grizzle. Asymptotic model matching for nonlinear systems. *IEEE Trans. Automat. Contr.*, 39:1539 – 1550, 1991.
- [7] S. Diop and M. Fliess. On nonlinear observability. page 152, 1991.
- [8] M. Fliess and S. T. Glad. An algebraic approach to linear and nonlinear control. pages 223–267, 1993.
- [9] K.M. Hangos and I.T. Cameron. *Process Modelling and Model Analysis*. Academic Press, London, 2001.
- [10] R.M. Hirschorn. Output tracking in multivariable nonlinear systems. *IEEE Trans. Automat. Contr.*, 26:593–595, 1981.
- [11] J. Huang and W.J. Rugh. On nonlinear multivariable servomechanism problem. *Automatica*, 26:963–972, 1990.
- [12] A. Isidori. The matching of a prescribed linear input–output behaviour in a nonlinear system. *IEEE Trans. Automat. Contr.*, 30:258–265, 1985.
- [13] J. Jin, S. Ko, and C.-K. Ryoo. Fault tolerant control for satellites with four reaction wheels. *Control Engineering Practice*, 16:1250–1258, 2008.
- [14] A. D. Kalafatis, L. Wang, and W.R. Cluett. Identification of wiener-type nonlinear systems in a noisy environment. *Int. J. Control*, 66:923–941, 1997.
- [15] A. A. Karve, R. Uddin, and J. J. Dorning. Stability analysis of BWR nuclear-coupled thermal-hydraulics using a simple model. *Nuclear Engineering and Design*, 177:155–177, 1997.
- [16] L. Keviczky, J. Bokor, and Cs. Bányász. A new identification method with special parametrization for model structure determination. pages 561–568, 1979.

- [17] L. Ljung. *System Identification - Theory for the User*. Prentice Hall, Englewood Cliffs, N.J., 1987.
- [18] L. Ljung. Perspectives on system identification. 2008. plenary lecture.
- [19] L. Ljung and T. Glad. On global identifiability of arbitrary model parametrizations. *Automatica*, 30:265–276, 1994.
- [20] G. Margaria, E. Riccomagno, M. J. Chappell, and H. P. Wynn. Differential algebra methods for the study of the structural identifiability of rational function state-space models in the biosciences. *Mathematical Biosciences*, 174:1–26, 2001.
- [21] P. P. Menon, I. Postlethwaite, S. Bennani, A. Marcos, and D. G. Bates. Robustness analysis of a reusable launch vehicle flight control law. *Control Engineering Practice*, in print:doi:10.1016/j.conengprac.2008.12.002, 2009.
- [22] D. Nesic and A.R. Teel. Input-output stability properties of networked control systems. *IEEE Transactions on Automatic Control*, 49:1650–1667, 2004.
- [23] Paks Nuclear Power Plant. VVER - 440/213 - the primary circuit. 2005. <http://www.npp.hu/mukodes/tipusok/primer-e.htm>.
- [24] R. H. Perry and D. W. Green. *Perry's Chemical Engineers' Handbook (7th edition)*. Mc Graw Hill, New York, 1999.
- [25] Pressurized water reactor simulator. IAEA-TCS-22, ISSN 1018-5518, IAEA, Vienna. 2003.
- [26] M. P. Saccomani, S. Audoly, and L. D'Angio. Parameter identifiability of nonlinear systems: the role of initial conditions. *Automatica*, 39:619–632, 2003.
- [27] Z. Szabó, P. Gáspár, and J. Bokor. Reference tracking of Wiener systems using dynamic inversion. pages on CD, paper ID: WeA06.5, 2005.
- [28] G. Szederkényi. Identifiability study of a pressurizer in a pressurized water nuclear power plant. 2009.

- [29] G. Szederkényi, Z. Szabó, J. Bokor, and K.M. Hangos. Analysis of the networked implementation of the primary circuit pressurizer controller at a nuclear power plant. pages 1604–1609, 2008. ISBN: 978-1-4244-2505-1.
- [30] M. Tabbara, D. Nesic, and A.R. Teel. Stability of wireless and wireline networked control systems. *IEEE Transactions on Automatic Control*, 52:1615–1630, 2007.
- [31] I. Varga, G. Szederkényi, K.M. Hangos, and J. Bokor. Modeling and model identification of a pressurizer at the paks nuclear power plant. pages 678–683, March 2006.
- [32] N. Vatanski, J.-P. Georges, C. Auburn, E. Rondeau, and S.-L. Jamsa-Jounela. Networked control with delay measurement and estimation. *Control Engineering Practice*, 17:231–244, 2009.
- [33] J. Voros. Identification of nonlinear dynamic systems using extended hammerstein and wiener models. *Control-Theory and Advanced Technology*, 10:1203–1212, 1995.
- [34] E. Walter. *Identification of State Space Models*. Springer, Berlin, 1982.
- [35] E. Walter. *Identifiability of Parametric models*. Pergamon Press, Oxford, 1987.
- [36] M. Wellers and N. Kositzka. Stable nonlinear model predictive control of constrained wiener and hammerstein models. *ISA-TECH auf Interkama 99, Düsseldorf*, pages 333–341, 1999.
- [37] D. Westwick and M. Verhaegen. Identifying mimo wiener systems using subspace model identification methods. *Signal Process.*, 52:235–258, 1996.
- [38] W. M. Wonham. *Linear Multivariable Control – A Geometric Approach*. 1985.
- [39] C. Fazekas, G. Szederkényi, and K.M. Hangos. A simple dynamic model of the primary circuit in VVER plants for controller design purposes. *Nuclear Engineering and Design*, 237:1071–1087, 2009.
- [40] C. Fazekas, G. Szederkényi, and K.M. Hangos. Parameter estimation of a simple primary circuit model of a VVER plant. *IEEE Transactions on Nuclear Science*, 55:2643–2653, 2008.